

Shape of the subducted Rivera and Cocos plates in southern Mexico: Seismic and tectonic implications

Mario Pardo¹ and Gerardo Suárez

Instituto de Geofísica, Universidad Nacional Autónoma de México

Abstract. The geometry of the subducted Rivera and Cocos plates beneath the North American plate in southern Mexico was determined based on the accurately located hypocenters of local and teleseismic earthquakes. The hypocenters of the teleseisms were relocated, and the focal depths of 21 events were constrained using a body wave inversion scheme. The subduction in southern Mexico may be approximated as a subhorizontal slab bounded at the edges by the steep subduction geometry of the Cocos plate beneath the Caribbean plate to the east and of the Rivera plate beneath North America to the west. The dip of the interplate contact geometry is constant to a depth of 30 km, and lateral changes in the dip of the subducted plate are only observed once it is decoupled from the overriding plate. On the basis of the seismicity, the focal mechanisms, and the geometry of the downgoing slab, southern Mexico may be segmented into four regions: (1) the Jalisco region to the west, where the Rivera plate subducts at a steep angle that resembles the geometry of the Cocos plate beneath the Caribbean plate in Central America; (2) the Michoacan region, where the dip angle of the Cocos plate decreases gradually toward the southeast, (3) the Guerrero-Oaxaca region, bounded approximately by the onshore projection of the Orozco and O'Gorman fracture zones, where the subducted slab is almost subhorizontal and underplates the upper continental plate for about 250 km, and (4) the southern Oaxaca and Chiapas region, in southeastern Mexico, where the dip of the subduction gradually increases to a steeper subduction in Central America. These drastic changes in dip do not appear to take place on tear faults, suggesting that smooth contortions accommodate these changes in geometry. The inferred 80 and 100 km depth contours of the subducted slab lie beneath the southern front of the Trans-Mexican Volcanic Belt, suggesting it is directly related to the subduction. Thus the observed nonparallelism with the Middle American Trench is apparently due to the changing geometry of the Rivera and Cocos plates beneath the North American plate in southern Mexico, and not to zones of weakness in the crust of the North American plate as some authors have suggested.

Introduction

The seismicity and tectonics of southern Mexico are characterized by the subduction of the oceanic Cocos and Rivera plates beneath the North American lithosphere along the Middle American Trench. Several studies have shown that this subduction zone exhibits lateral variations in the dip of the subducted oceanic lithosphere [e.g., Molnar and Sykes, 1969; Stoiber and Carr, 1973; Dean and Drake, 1978; Nixon, 1982; Bevis and Isacks, 1984; Burbach *et al.*, 1984; Ponce *et al.*, 1992]. A steep subduction geometry in southeastern Mexico [Ponce *et al.*, 1992] and in the Jalisco region of western Mexico [Pardo and Suárez, 1993] bound a slab dipping apparently at a very shallow angle in central Mexico.

On the basis of teleseismic data, Burbach *et al.* [1984] concluded that the subducted Cocos plate can be divided into these three major regions dipping at different angles. Bevis and Isacks [1984], using a hypocentral trend surface analysis, find no evidence of tear faulting separating these segments of the subducted lithosphere and suggested that the transition

takes place on a fold. They also suggested that to the southeast, the change in dip may be related to differences in the age of oceanic lithosphere on either side of the Tehuantepec ridge.

Until recently, the accepted view was that the Cocos plate subducts beneath central Mexico at a constant and relatively shallow angle of ~ 12 to 15° [Stoiber and Carr, 1973; Hanus and Vanek, 1978; Havskov *et al.*, 1982; Burbach *et al.*, 1984; Bevis and Isacks, 1984; Singh and Mortera, 1991]. Using data from a permanent local network, Suárez *et al.* [1990] defined the geometry of the subducted plate in more detail and showed that in central Mexico the slab does not subduct at a steady shallow angle. Instead, after an initial dip of $\sim 15^\circ$, the slab becomes almost subhorizontal and underplates the North American upper lithosphere. This plate geometry is reminiscent of that found in central Peru and central Chile, where the Nazca plate also subducts horizontally beneath the South American upper lithosphere.

Perhaps one of the more striking tectonic features in southern Mexico is the location of the Trans-Mexican Volcanic Belt. The Trans-Mexican Volcanic Belt crosses southern Mexico from east to west at about 19°N . The distribution of the volcanic arc is oblique ($\sim 16^\circ$) relative to the Middle American Trench (Figure 1), in an unusual geometry which is not parallel to the subduction zone. The Trans-Mexican Volcanic Belt is ~ 100 km wide and is cut by a sequence of grabens that are oblique relative to the general trend of the arc [Nixon, 1982].

¹Now at Departamento de Geofísica, Universidad de Chile, Santiago.

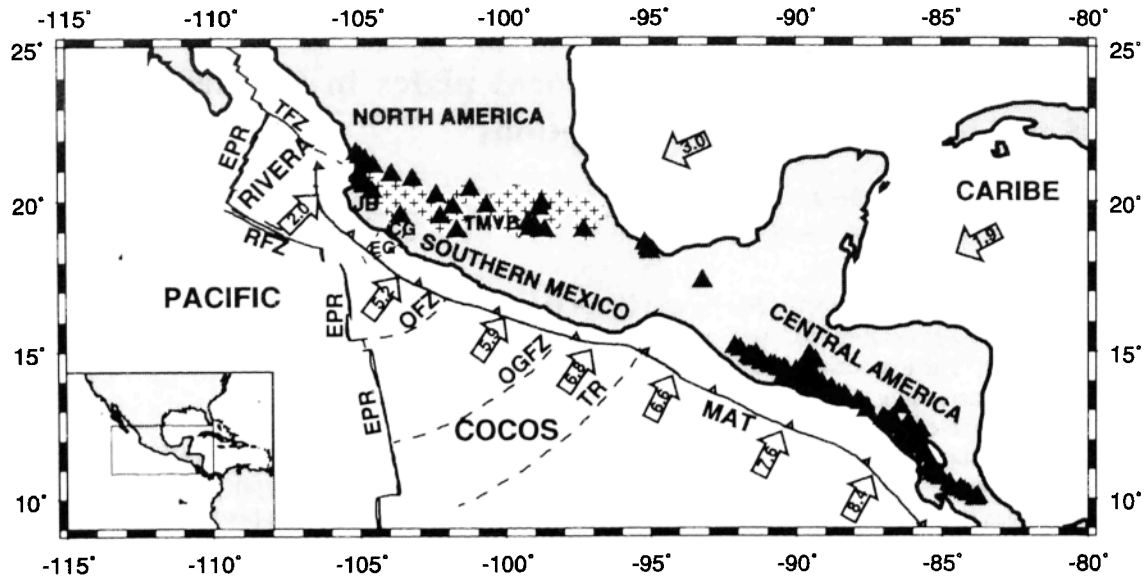


Figure 1. General tectonic setting of the study area. Five lithospheric plates are shown: Pacific, Rivera, Cocos, North America, and Caribbean. Relative convergence rates (cm/yr) between the oceanic and continental plates are indicated by open arrows, and absolute motions of the upper plates relative to a hot spot frame of reference are shown by shaded arrows. The abbreviations are EPR, East Pacific Rise; TFZ, Tamayo Fracture Zone; RFZ, Rivera Fracture Zone; OFZ, Orozco Fracture Zone; OGFZ, O'Gorman Fracture Zone; TR, Tehuantepec Ridge; MAT, Middle American Trench; JB, Jalisco Block; CG, Colima Graben; EG, El Gordo Graben. Solid triangles indicate Quaternary volcanism, and the crossed area indicates the Trans-Mexican Volcanic Belt (TMVB).

The volcanic arc erupted since the Miocene and mostly during the Pliocene and Quaternary. A diversity of structures such as large strato-volcanoes, monogenetic cinderic cones, shield volcanoes, and several calderas are found on the volcanic belt. The chemical and petrological characteristics of the Trans-Mexican Volcanic Belt indicate that, in general, the volcanic sequences that form this belt are calc-alkaline, although some localized zones of alkaline volcanism exist along the Trans-Mexican Volcanic Belt, especially in western Mexico [e.g., Luhr *et al.*, 1985; Allan *et al.*, 1991]. The radiometric dating of volcanic rocks and the broad nature of the Trans-Mexican Volcanic Belt suggest the migration of volcanism toward the trench since 5.3 Ma [Delgado *et al.*, 1993].

A number of contrasting hypotheses have been proposed to account for the nonparallelism of the Trans-Mexican Volcanic Belt relative to the Middle American Trench and its relation to the subducted oceanic plate. These hypotheses can be divided into two groups: (1) those which favor a direct association between subduction and volcanism [e.g., Molnar and Sykes, 1969; Demant and Robin, 1975; Nixon, 1982; Burbach *et al.*, 1984; Suárez and Singh, 1986], and (2) those which suggest that the Trans-Mexican Volcanic Belt bears no direct tectonic relation with the subduction along the Middle American Trench and explain its origin as resulting from zones of weakness within the crust of southern México, inherited from earlier episodes of deformation [e.g., Mooser, 1972; Gastil and Jensky, 1973; Shurbet and Cebull, 1973; Johnson and Harrison, 1989].

An integral study that takes into account the geometry of the subducted Rivera and Cocos plates beneath the North American lithosphere (NW of 94°W), the stress distribution in the subducted slab, and the relation between the subduction process and the anomalous location of the Trans-Mexican

Volcanic Belt is presented here. The availability of data from permanent and temporary local networks and the occurrence of recent earthquakes recorded at teleseismic distances which had not been studied previously offer an excellent opportunity to understand this region of complex subduction geometry in greater detail.

The purpose of this study is to determine the geometry of the subducted Cocos and Rivera plate, based on all the available and reliable hypocenter locations of earthquakes recorded with local and teleseismic networks, and to study the regional distribution of stresses with reported and newly determined focal mechanisms. Together, these data are analyzed to determine an integral model of the subduction in southern Mexico and its implications on the seismicity and tectonics of the area.

Tectonic Setting

This study includes the subduction of the Rivera and Cocos plates in southern Mexico, west of the intersection of the Tehuantepec ridge with the Middle American Trench (Figure 1). According to Mammerickx and Klitgord [1982], the tectonic history of this region for the last 25 m.y. has suffered at least three major plate reorganizations. The old Farallon plate evolved first to the Guadalupe plate, which was later segmented into the actual Rivera and Cocos plates. The position of the spreading centers moved east, from about 12.5 to 11 Ma, to the Mathematician seamounts. Later, between 6.3 to 3.5 Ma, it shifted to its actual position of the East Pacific Rise (EPR).

Rivera Plate

The existence of the small Rivera plate was first suggested by Atwater [1970]. Since then, several authors have shown

that the Rivera plate is kinematically distinct from the North American and Cocos plates [Bandy and Yan, 1989; Eissler and McNally, 1984; DeMets and Stein, 1990]. The junction between the East Pacific rise and Rivera fracture zone is located 165 km to the west of the Middle American Trench [Bourgois and Michaud, 1991]. The precise location of the Rivera-Cocos boundary is still controversial, and no clear bathymetric features can be associated to a distinct and clear plate boundary [Eissler and McNally, 1984; Mammerickx, 1984; Bourgois and Michaud, 1991]. Bandy [1992] suggested that the El Gordo graben may be part of the Rivera-Cocos plate boundary (Figure 1).

The Rivera lithosphere consumed at the trench is of late Miocene age (~9 Ma) [Klitgord and Mammerickx, 1982]. Although the seismicity related to the subduction of the Rivera plate beneath the Jalisco block is low (Figure 2), at least six large earthquakes ($M_s > 7.0$) have been documented since 1837, including the great 1932 Jalisco earthquake ($M_s=8.2$) [Eissler and McNally, 1984; Singh et al., 1985]. This contradicts the suggestion that the Rivera plate subducts aseismically [Nixon, 1982]. On the basis of locally recorded microearthquakes and relocated hypocenters of teleseismic events, Pardo and Suárez [1993] concluded that the subduction of the Rivera plate takes place with a steep angle (~50°) below depths of 40 km.

Cocos Plate

The Cocos plate subducts at a rate that increases to the southeast from 4.8 cm/yr at 104.5°W to 7.5 cm/yr at 94°W [DeMets et al., 1990]. The age of the Cocos plate also varies along the Middle American Trench, with jumps associated to fracture zones (Figure 1). To the east, the Tehuantepec ridge intersects the Middle American Trench near ~95°W. This ridge is the largest linear bathymetric feature on the eastern flank of the East Pacific Rise. Apparently, it is the morphological expression of a fracture zone that presumably separates crust of significantly different ages. A younger and shallower crust to the northwest differs in age to that southeast of the Tehuantepec ridge by approximately 10 to 25 m.y. [Couch and Woodcock, 1981].

Data Used in the Analysis

The data used to infer the morphology of the subducted Rivera and Cocos plates beneath southern Mexico are (1) accurately determined hypocenters obtained from local microearthquake data recorded by permanent and temporary seismological stations, and (2) events recorded at teleseismic distances and relocated using the method of Joint Hypocenter Determination (JHD) [Dewey, 1971]. For some of the larger events ($m_b \geq 5.0$), the focal depth was constrained from the inversion of long-period body waves [Nábelek, 1984].

Local Microearthquake Data

All the available local data from the permanent and temporary seismic networks installed in southern Mexico were used in order to accurately locate the hypocenters of microearthquakes within the zone [Nava, 1984; UNAM Seismology Group, 1986; Sansores, 1990; Pardo and Suárez, 1993; Ponce et al., 1992; Zuñiga et al., 1993].

The hypocenters were located using HYPO71 [Lee and Valdes, 1985] with the velocity model reported by Suárez et al. [1992], and a velocity ratio ($V_p/V_s = 1.76$) determined for the

Guerrero region. Hypocentral locations were considered reliable and included in the final dataset when they met the following criteria: (1) a minimum of seven phase readings with at least one S wave arrival time; (2) a root mean square error of less than 0.25 s; (3) estimated hypocentral errors of less than 10 km; (4) a hypocentral variation of less than 10 km when the initial trial depth was varied from 10 to 150 km; and (5) a maximum angle gap between the epicenter and the local stations of less than 230°. From a total of over 3000 events, a final subset of only 1101 hypocenters satisfied these criteria (Figure 2).

Relocated Earthquakes

Earthquakes with magnitude $m_b > 4.5$ were relocated in southern Mexico, using the JHD method [Dewey, 1971] and the phase readings reported by the International Seismological Centre (ISC) between 1964 and January 1990. Several calibration events were used along the region: (1) for the zone between 103° and 105°, we used the largest aftershock of the 1973 Colima earthquake ($M_s=7.5$). This aftershock ($M_s=6.2$) was located with a temporary seismic network deployed after the mainshock [Reyes et al., 1979]; (2) for the zone between 100° and 103°W, the 1979 Petatlan earthquake ($M_s=7.8$) recorded with portable stations [Valdés et al., 1982] was used; and (3) the 1981 Ometepepec earthquake ($M_s=7.2$) [Nava, 1984] for the easternmost region.

The JHD method [Dewey, 1971] determines relocated hypocenters relative to the hypocenter of the calibration event, applying time adjustments to the phase readings of P , pP , and S . These time adjustments of the reporting seismological stations were obtained from the variance of the different phase arrival times of the calibration events and from the earthquakes reported in this study for which the focal depth was constrained using a long-period body wave inversion. These calibration station-phases were then used in a single-event location method [Dewey, 1971], in order to determine the relocated hypocenters within the zones of each calibration event. A spherical Earth model was used in the JHD method to relocate the hypocenters.

For the eastern part of the region, we used the relocated hypocenters obtained by M. Cruz and G. Suárez (manuscript in preparation) who applied a similar procedure. The precision of each relocated hypocenter relative to the calibration event is estimated by computing error ellipsoids for the hypocentral coordinates at a 90% confidence level. A hypocentral location was considered reliable when the ellipsoid semiaxes were less than 20 km; all events which did not meet these criteria were discarded. A final subset of 207 reliable hypocenters was obtained from an initial set of over 300 events. The hypocentral and focal parameters of all the earthquakes studied are shown on Figure 2 and provided as an electronic supplement for the reader.

Long-Period Body Wave Inversion

The formal inversion of P , SV , and SH waveforms constrains the focal mechanism and the centroidal focal depth [Nábelek, 1984]. Long-period seismograms of teleseismic earthquakes ($25^\circ \geq \Delta \geq 90^\circ$) from the Global Digital Seismograph Network (GDSN) were used for the events that occurred between 1980 and 1987 and from the World-Wide Standardized Seismograph Network (WWSSN) for the events that occurred prior to 1980. The analog seismograms were

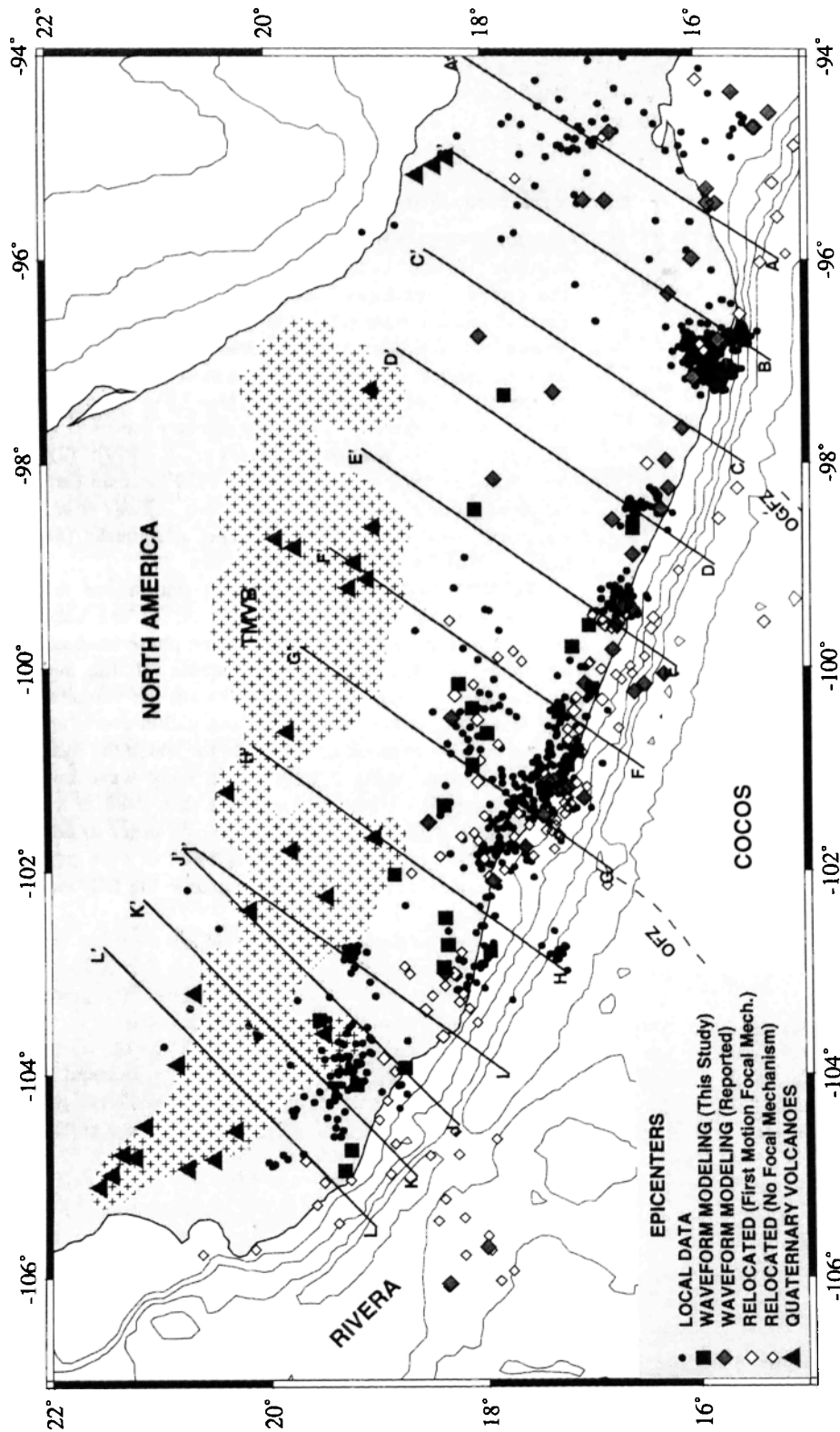


Figure 2. Epicenters of the earthquake data set used in this study. Solid dots indicate microearthquakes located using local data; their locations on the map reflect the regions covered by local networks. Solid squares are relocated events for which the focal depth was constrained by body wave inversion [Nábelek, 1984]. Relocated hypocenters obtained from the Joint Hypocenter Determination method [Dewey, 1971] are shown as relocated epicenters with reported focal mechanisms based on body wave modeling (large and solid diamonds); epicenters with focal mechanism determined from first motion *P* waves (gray intermediate size diamonds); and epicenters of events without focal mechanism (open small diamonds). The cross sections shown on Figure 4 are oriented in the direction of relative plate convergence. Other symbols are as on Figure 1.

hand-digitized and filtered with a high-pass filter with cutoff frequency of 0.017 Hz (60 s) to eliminate long-period noise. All of the events modeled are in the magnitude range $5.0 \geq m_b \geq 6.1$, and therefore a point source was assumed in all cases. Key examples of the modeled events are shown on Figure 3.

Analysis of Hypocentral Data

In plan view, the seismicity of southern Mexico shows a distribution in bands parallel to the trench [Suárez *et al.*, 1990] (Figure 2). The first band along the coast is related to the interplate seismogenic contact. North of it lies an almost aseismic zone, which becomes broader between 96°W and 101°W. Farther inland, a second band of deeper intraplate events (depths > 50 km) in the oceanic downgoing slab lies at a distance of 150–250 km from the trench (Dt). Beyond this last band, which lies immediately to the south of the Trans-Mexican Volcanic Belt, the seismic activity disappears.

In order to map the geometry of the subducted slab, 12 cross sections of the seismicity were drawn (Figures 2 and 4). The origin of all the cross sections is the trench, and they are all oriented in the direction of convergence predicted between the Rivera-North America [DeMets and Stein, 1990] and Cocos-North America [DeMets *et al.*, 1990] plate pairs (Figure 2).

The shallow part of the subduction zone ($h < 30$ km) indicates a constant interplate geometry that initially dips at ~10° and gradually increases to ~25° at a depth of 30 km (Figure 4). This geometry is observed throughout the subduction zone in southern Mexico and appears to be independent of the age and the relative convergence velocity of the subducted oceanic plate; no lateral changes of the interplate geometry are observed where major bathymetric features are being subducted.

Geometry of the Subducted Plate

The subducted Rivera and Cocos plates show rapid lateral variations in dip at depths greater than ~30 km (Figure 4). In the Isthmus of Tehuantepec (cross section AA' on Figures 2 and 4a), the seismicity defines a Wadati-Benioff zone dipping at an angle of ~30°. Immediately toward the west (Figure 4b), the dip of the downgoing slab is shallower and decreases to an angle of ~25°. In central Mexico, the geometry of the downgoing slab becomes almost subhorizontal at distances of between 110 km to 275 km from the trench and at depths of about 50 km (Figures 4c to 4g). A similar geometry was inferred for the Guerrero region (Figures 4f and 4g) by Suárez *et al.* [1990] and Singh and Pardo [1993] using local data.

In the westernmost region of the Cocos plate (Figures 4h and 4i), the dip of the subducted slab changes again rapidly from the subhorizontal subduction observed in the region of Guerrero and Oaxaca (Figures 4c to 4g) to a steeper dip of ~30°. This dip angle is similar to that observed on Figure 3a, near the Isthmus of Tehuantepec. Toward the northwest, the slab continues to steepen progressively, and beneath the Colima volcano, the Wadati-Benioff is clearly followed dipping at an angle of ~50° down to a maximum depth of approximately 130 km (Figure 4j).

A cross section parallel to the trench, from (19°N, 106°W) to (15°N, 95°W), shows the rapid and drastic variations in maximum depth extent of the hypocenters within southern Mexico (Figure 5). In the case of the Rivera plate beneath the Jalisco region, the maximum focal depth is 130 km. Toward

the southeast, the maximum depth observed for earthquakes in the Cocos plate, between the El Gordo graben and the point where the Orozco Fracture Zone apparently intersects the trench, is 100 km. Farther east, in the region bounded approximately by the onshore projection of the Orozco and the O'Gorman fracture zones, where a good coverage of local stations exists, the maximum focal depths observed are consistently less than 70 km. Between the O'Gorman fracture zone and the Tehuantepec Ridge the maximum depth of earthquakes increases continuously down to depths of 180 km. The depth extent of the various segments of the subduction zone directly correlates with the observed dip of the slab.

Smooth contours of the Wadati-Benioff zone were obtained using a two-dimensional spline interpolation [Smith and Wessel, 1990] (Figure 6). In central Mexico, however, to the north of 18°N and at distances beyond 300 km from the trench, there is a remarkable dearth of seismic events (Figures 2 and 6). Thus the 80- and 100-km-deep contours cannot be mapped directly in central Mexico.

These two contours were drawn following the trend of the slab at shallower depths and extrapolating their location from the regions where they are well defined by the seismicity: to the west of 103°W and east of 96°W (Figure 6). The resulting contours show that the Cocos plate lies at depths of 80 to 100 km beneath the southern front of the Trans-Mexican Volcanic Belt (Figure 6). This depth of the Wadati-Benioff zone of approximately 100 km beneath the volcanic arc is observed in most subduction zones of the world. This suggests that the Trans-Mexican Volcanic Belt is directly related with the subduction of the oceanic slab beneath the North American plate and that the observed nonparallelism of the volcanic belt with the trench is mainly due to the geometry of the subducted plate.

Focal Mechanisms and State of Stress

In this study, 21 new focal mechanisms of earthquakes within the subducting Cocos plate are reported (see electronic supplements). The lower hemispheric projection of the focal mechanisms obtained from a waveform inversion reported in this study and in previous works are shown on Figure 7, and several key examples of the earthquakes modeled in this study are shown on Figure 3. These focal mechanisms are also shown on lateral projection on the cross sections (Figure 4). Owing to the absence of seismic stations to the south and west of southern Mexico, the focal mechanisms of small earthquakes reported from the first motion of *P* waves are poorly constrained. Therefore only one mechanism from first motion data alone was used; its small magnitude precluded the use of a formal inversion scheme (event 67 on the electronic supplement¹).

In a manner analogous to the seismicity, the stress pattern observed along the subduction zone may be divided in zones

¹An electronic supplement of this material may be obtained on a diskette or Anonymous FTP from KOSMOS.AGU.ORG. (LOGIN to AGU's FTP account using ANONYMOUS as the username and GUEST as the password. Go to the right directory by typing CD APEND. Type LS to see what files are available. Type GET and the name of the file to get it. Finally, type EXIT to leave the system.) (Paper 95JB00919, Shape of the subducted Rivera and Cocos Plates in southern Mexico: Seismic and tectonic implications, by Mario Pardo and Gerardo Suárez). Diskette may be ordered from American Geophysical Union, 2000 Florida Avenue, N.W., Washington, DC 20009; \$15.00. Payment must accompany order.

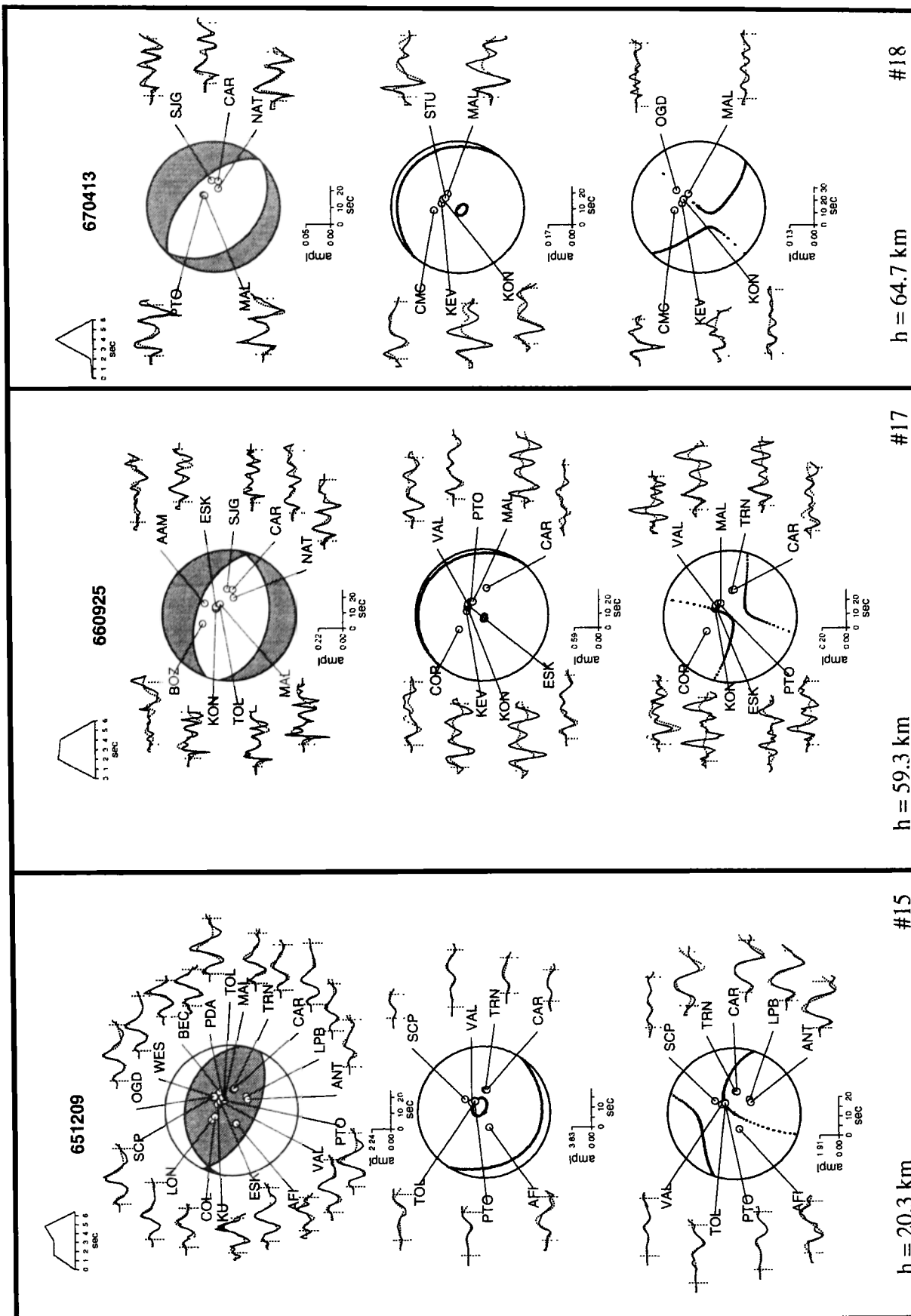


Figure 3. Focal parameters of selected events determined in this study. The focal mechanisms and depths of 21 earthquakes were determined using a formal inversion of long-period teleseismic P , SV , and SH waveforms [Nábelek, 1984]. The results are shown for 12 selected earthquakes representative of the data quality and focal parameters. Seismograms from the Global Digital Seismograph Network (GDSN) were used for the event that occurred after 1980 and from the World-Wide Standardized Seismograph Network (WSSN) for the events prior to this date. The magnitude of all the events is within $5.0 \leq m_b \leq 6.1$, and a point source was used in all the inversions. The focal mechanisms are shown in a lower hemispheric projection. Observed (solid line) and synthetic (dashed line) waveforms of (top) P wave, (middle) SV wave and (bottom) SH wave are also shown. The date of the event and the source time function are shown at the top. The centroidal depth and the event number are at the bottom.

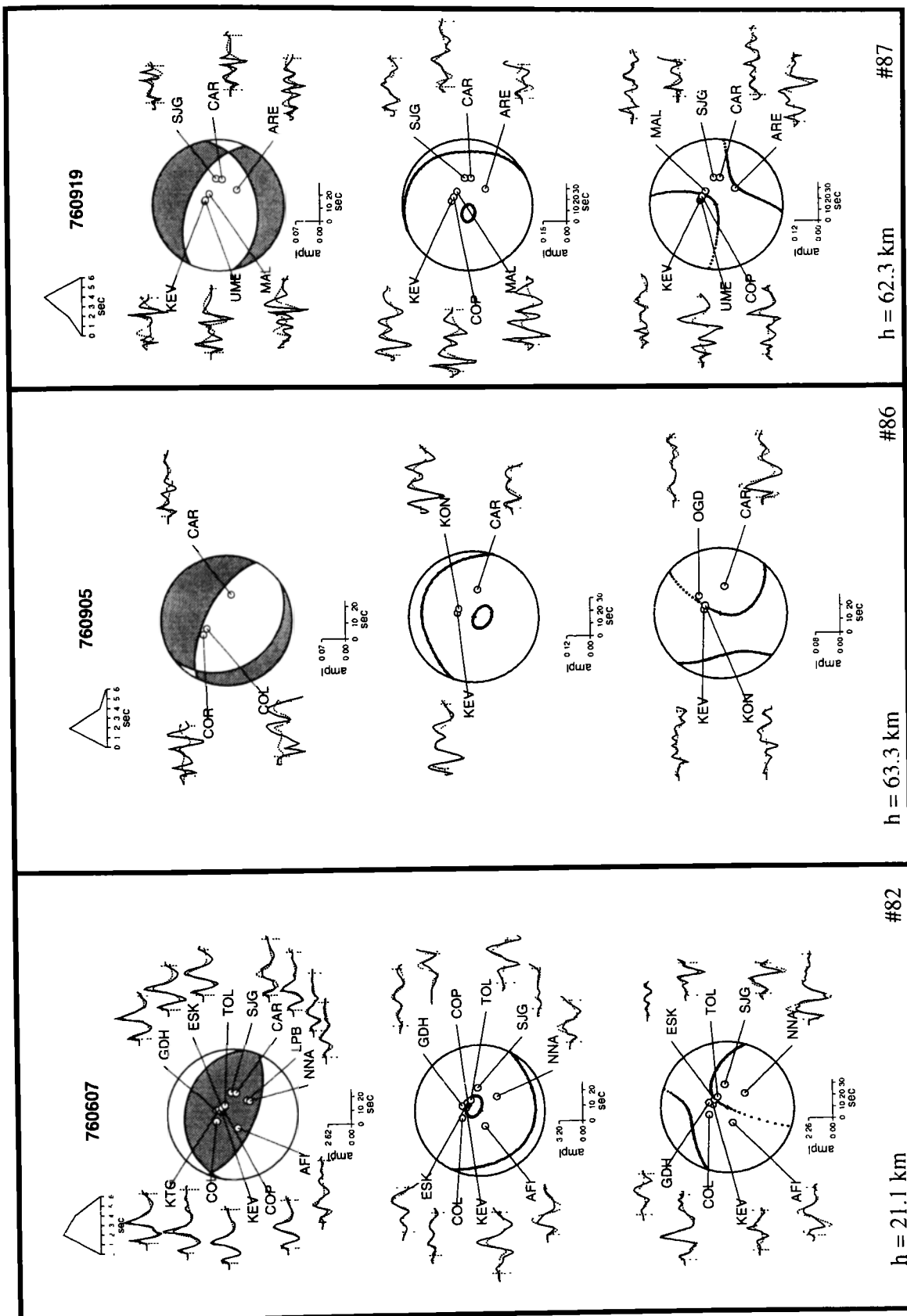


Figure 3. (continued)

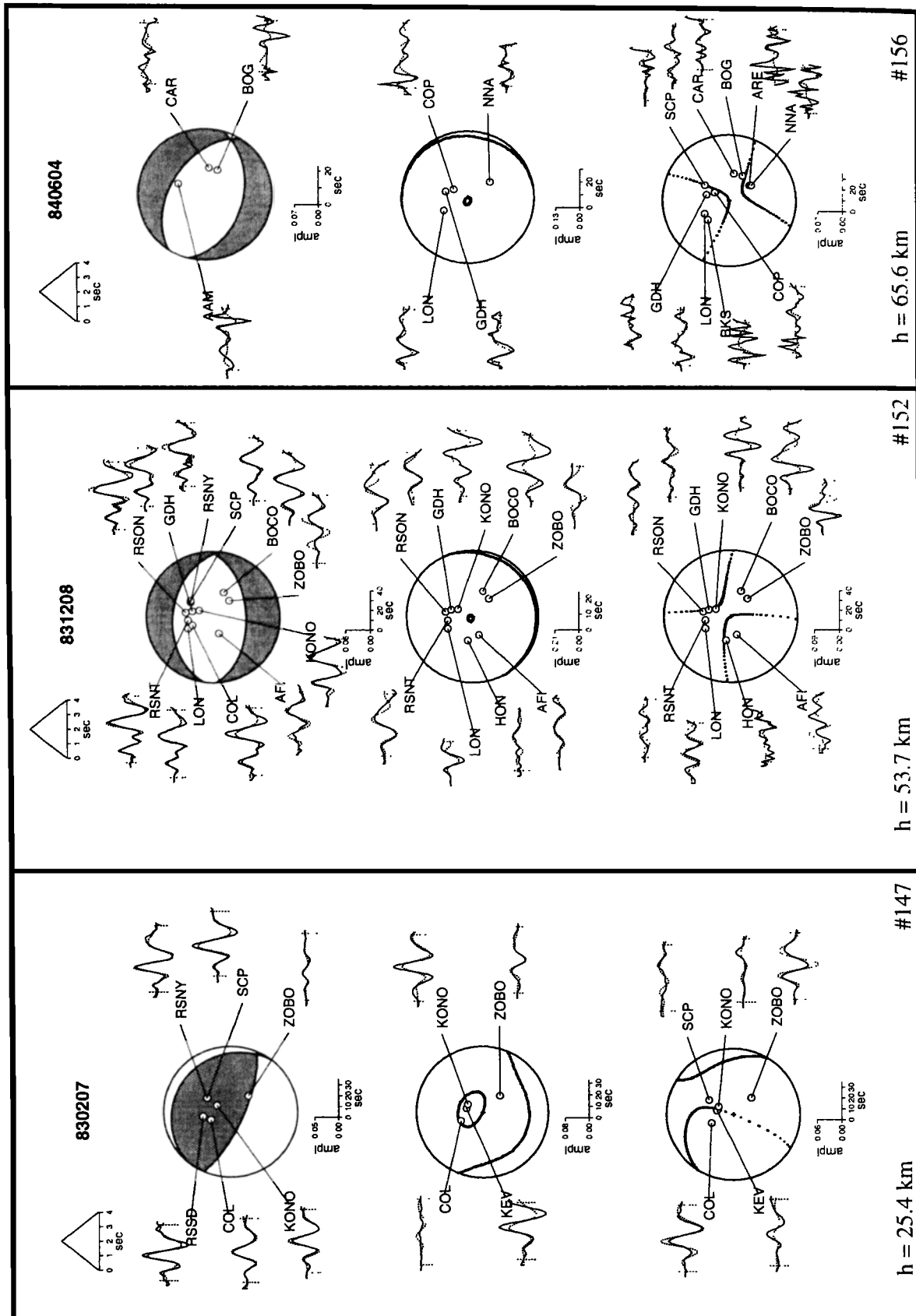
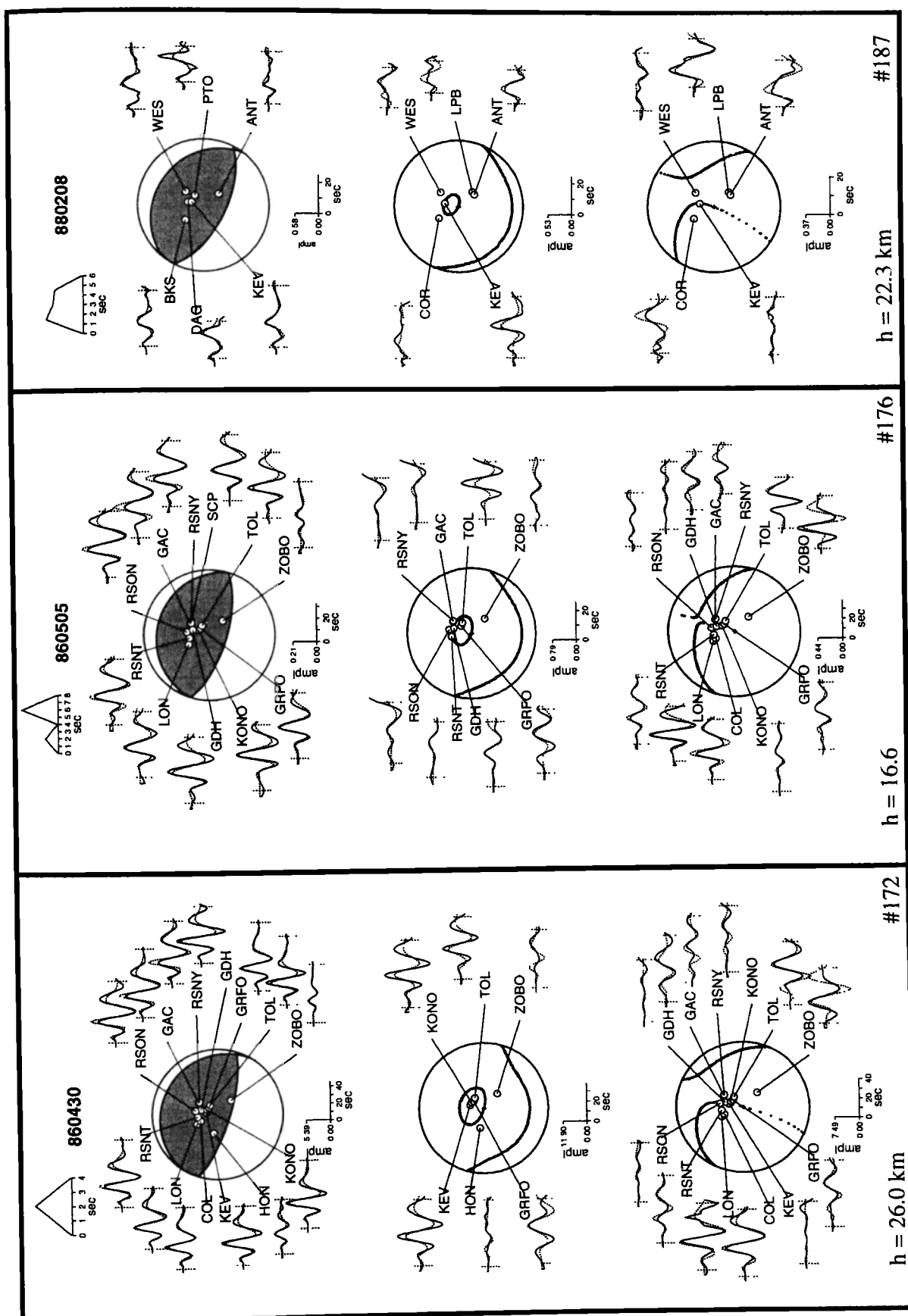


Figure 3. (continued)



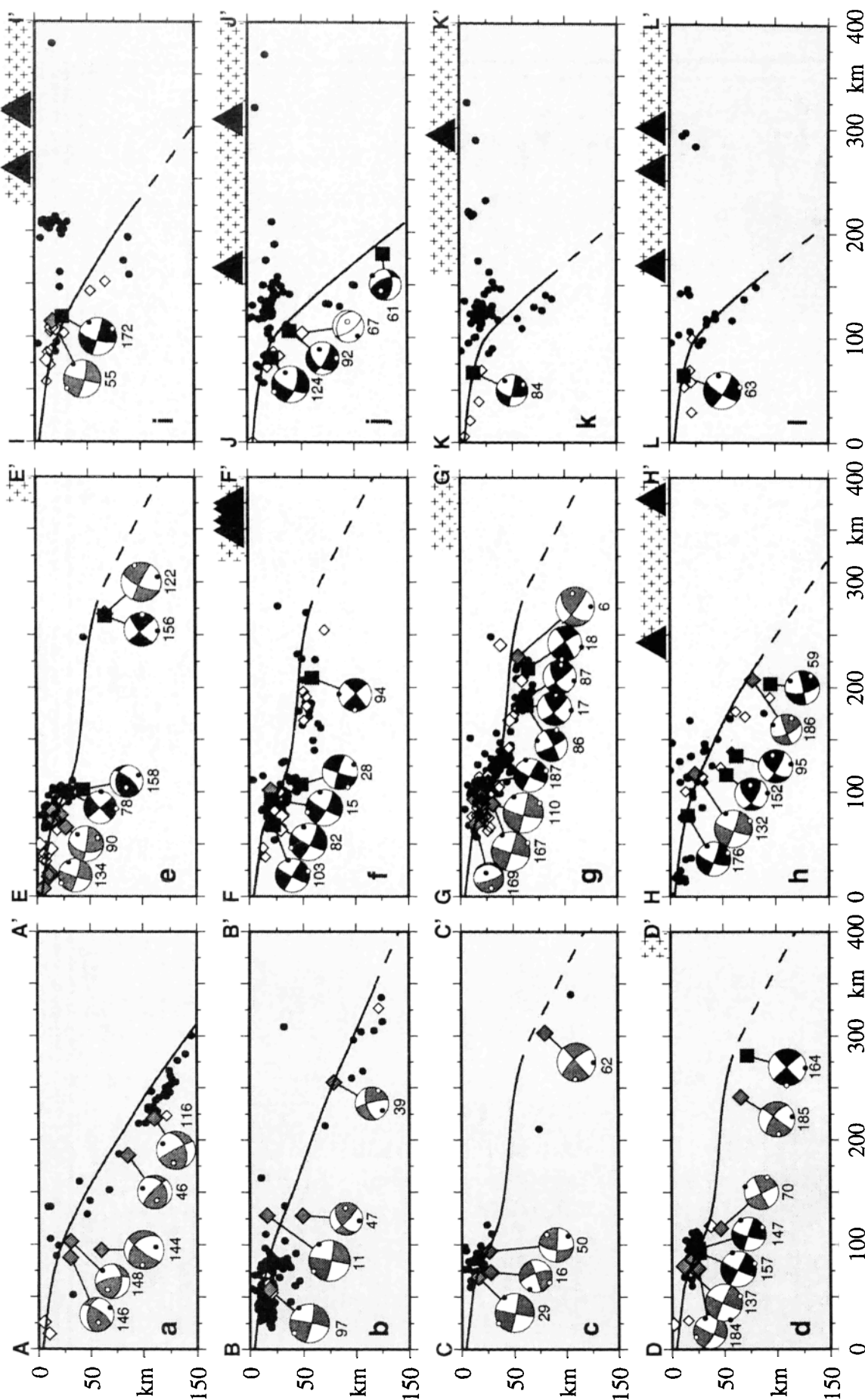


Figure 4. Cross sections shown on Figure 2. The symbols of the earthquakes projected on the cross sections are as on Figure 2. Focal mechanisms are shown on a side-looking, lower hemispheric projection where dark quadrants indicate compressional first motions. Focal mechanisms shown solid are from body wave inversions presented in this study, and those shown in dark gray are from body wave modeling results reported elsewhere. Numbers of the focal mechanisms are keyed to those in the electronic supplement. The top of the downgoing plate is shown on each cross section with a solid line; a dashed line is shown where it is extrapolated. The location of the Quaternary volcanoes (solid triangles) and of the Trans-Mexican Volcanic Belt (crossed area) are also shown in the cross sections.

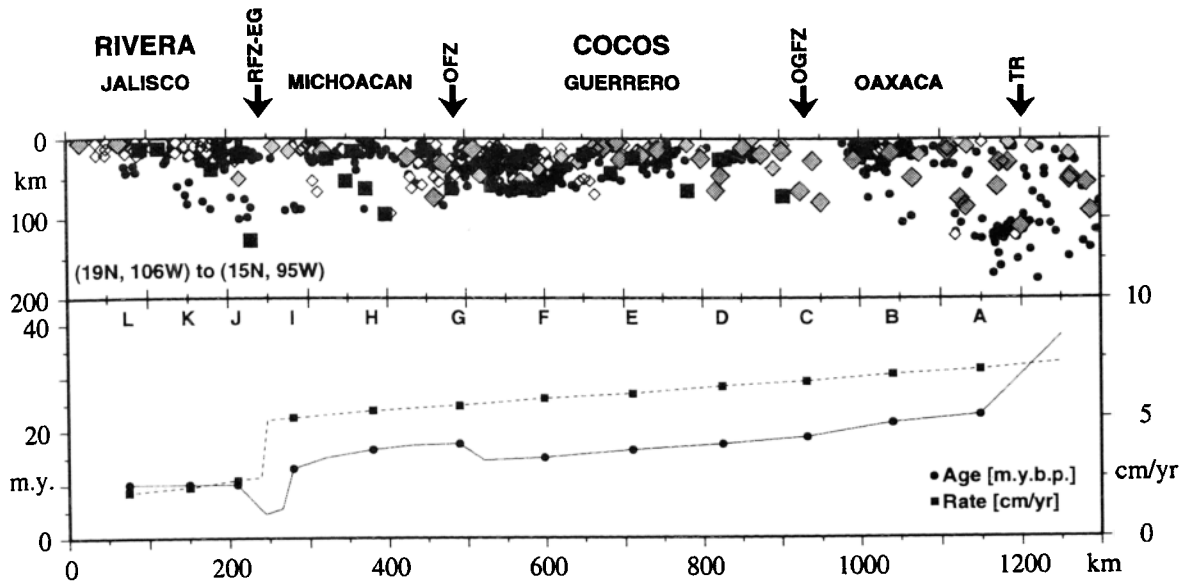


Figure 5. Relocated hypocenters projected onto a cross section parallel to the trench, from (19°N, 106°W) to (15°N, 95°W); symbols as on Figure 1. Southern Mexico can be separated into four major segments: Jalisco, Michoacan, Guerrero, and Oaxaca. The bottom part shows the variations in age of the subducted slab at the trench [Klitgord and Mammerickx, 1982] and in the rate of relative motion of the oceanic plates at the trench [DeMets and Stein, 1990, DeMets et al., 1990]. Cross sections A to L are those shown on Figures 2 and 4.

parallel to the trench (Figures 4 and 7). A shallow depth zone close to the trench shows interplate thrust faulting followed by downdip, normal faulting events. The thrust earthquakes are observed down to a maximum depth of ~25 km along the Cocos plate (Figure 4).

Downdip from the interplate contact, a zone of low seismic activity is observed which is followed farther inland by an area of intraplate events showing normal faulting at depths greater than 50 km. The normal faulting events in the downgoing slab (Figure 7) show, in general, *T* axes oriented in a direction parallel to the gradient of the subducted oceanic plate (Figure 6). Only where the slab shows a rapid change in dip, near 96°W and 101°W, the stress distribution become more complex (Figure 8).

Beneath the normal faulting events near the coastline, there is a sheet of compressional events, with depths ranging from 40 km to 50 km (events 47, 70, 158, 28, 152 and 67 on the electronic supplement; Figures 4b, 4d, 4e, 4f, 4h and 4j). This double zone in stress is probably associated to flexural stresses associated to the slab bending upward to become subhorizontal [Suárez et al., 1990].

Practically no crustal seismicity is observed in the overriding plate over the subducted Cocos plate (Figure 4). In contrast, there is a relatively high crustal seismicity within the Jalisco region in western Mexico (Figures 2 and 4j-4l), suggesting that the deformation of the Jalisco block is greater than that observed in the North American plate over the Cocos slab [Pardo and Suárez, 1993].

Discussion

Although the conditions controlling the geometry of subduction zones are still controversial, several authors have suggested that the principal factors affecting the geometry of a

subduction zone are the relative convergence rate in the subduction zone, the age of the subducted slab, the absolute motion of the overriding plate, and the subduction of aseismic bathymetric features, like ridges or intraplate seamounts [e.g., Cross and Pilger, 1982; Jarrard, 1986]. Except for the age of the slab, all of these parameters correlate negatively with the dip of the downgoing plate. Thus young lithosphere is apparently more buoyant than old plates and subducts at a lower dip angle.

Therefore, according to these empirical relations, the shallow dip observed in the subduction zone of southern Mexico could be explained by the relatively young age of the subducting slab, its moderate convergence rate, and the rapid absolute motion of the upper North American plate relative to the trench (Figure 1). To the east of the Tehuantepec ridge, where the Cocos plate subducts beneath the Caribbean plate with a steeper dip angle, the subducting slab is 10 to 25 m.y. older than to the west of TR [Couch and Woodcock, 1981], and the relative motion of the upper Caribbean plate toward the trench is lower than to the northwest [Gripp and Gordon, 1990] (Figure 1).

Southwestern Mexico is the region of the subduction zone where the Cocos plate is youngest. In this same manner, the age of the subducting Rivera plate is also relatively young. However, the dip of the downgoing slab in this area is steep. Thus the simple correlation between the age of the slab and its dip does not hold in this case. The only major difference between the Rivera and the Cocos subduction zones is the slow convergence rate between the Rivera and North American plates (~2 cm/yr) [DeMets and Stein, 1990], relative to a greater Cocos-North America convergence rate (~6 cm/yr) [DeMets et al., 1990] (Figures 1 and 4). Perhaps this low rate of relative motion becomes an important parameter affecting the geometry of the subducted Rivera plate.

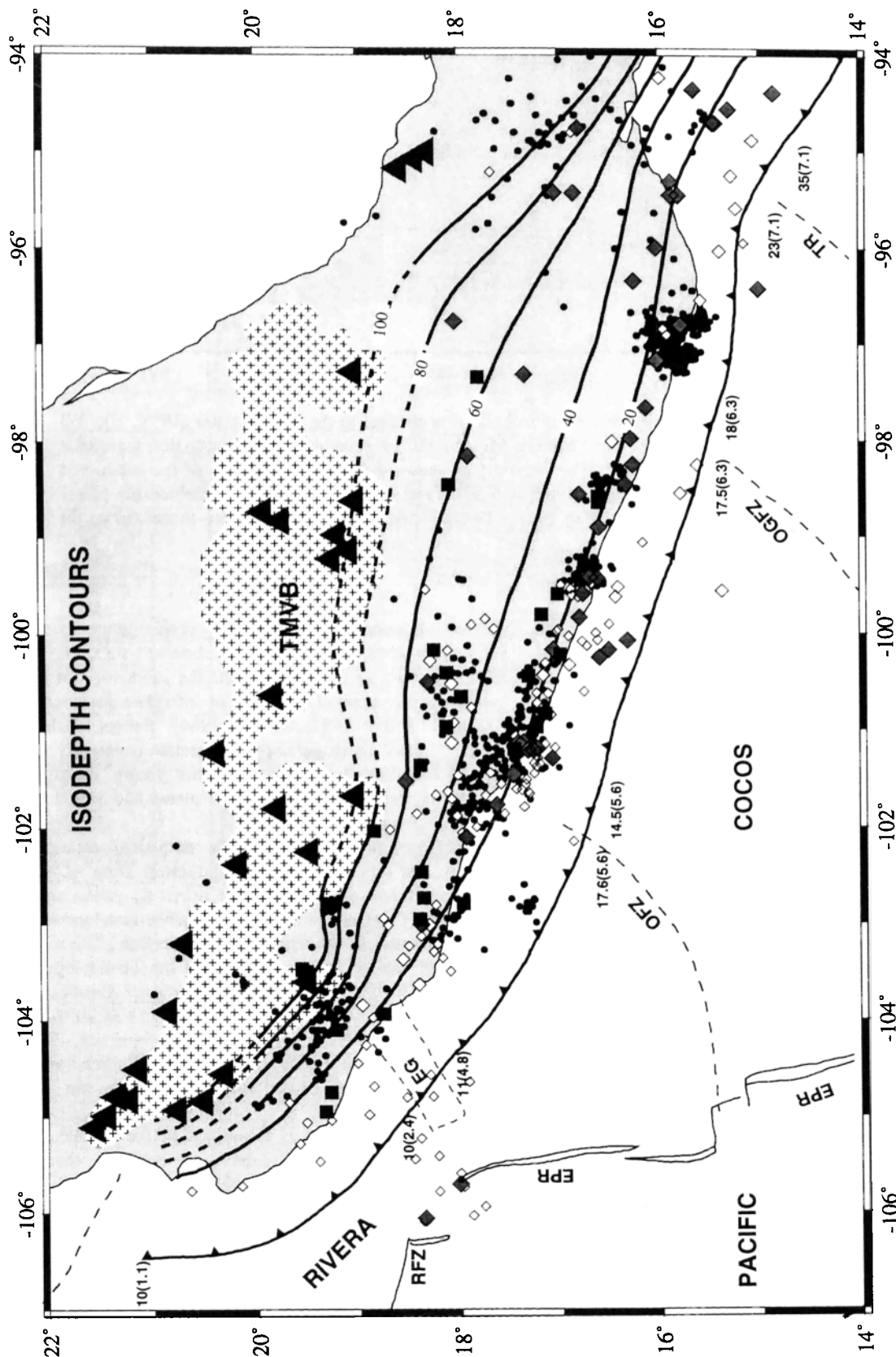


Figure 6. Isodepth contours of the subducted oceanic slab beneath the North American plate in southern Mexico drawn using a spline interpolation. Dashed lines indicate where the contours were extrapolated because no hypocentral data are available. Other symbols as on Figure 1. The age (Ma) of the oceanic slab and the convergence rate in parentheses (cm/yr) are shown along the Middle American Trench.

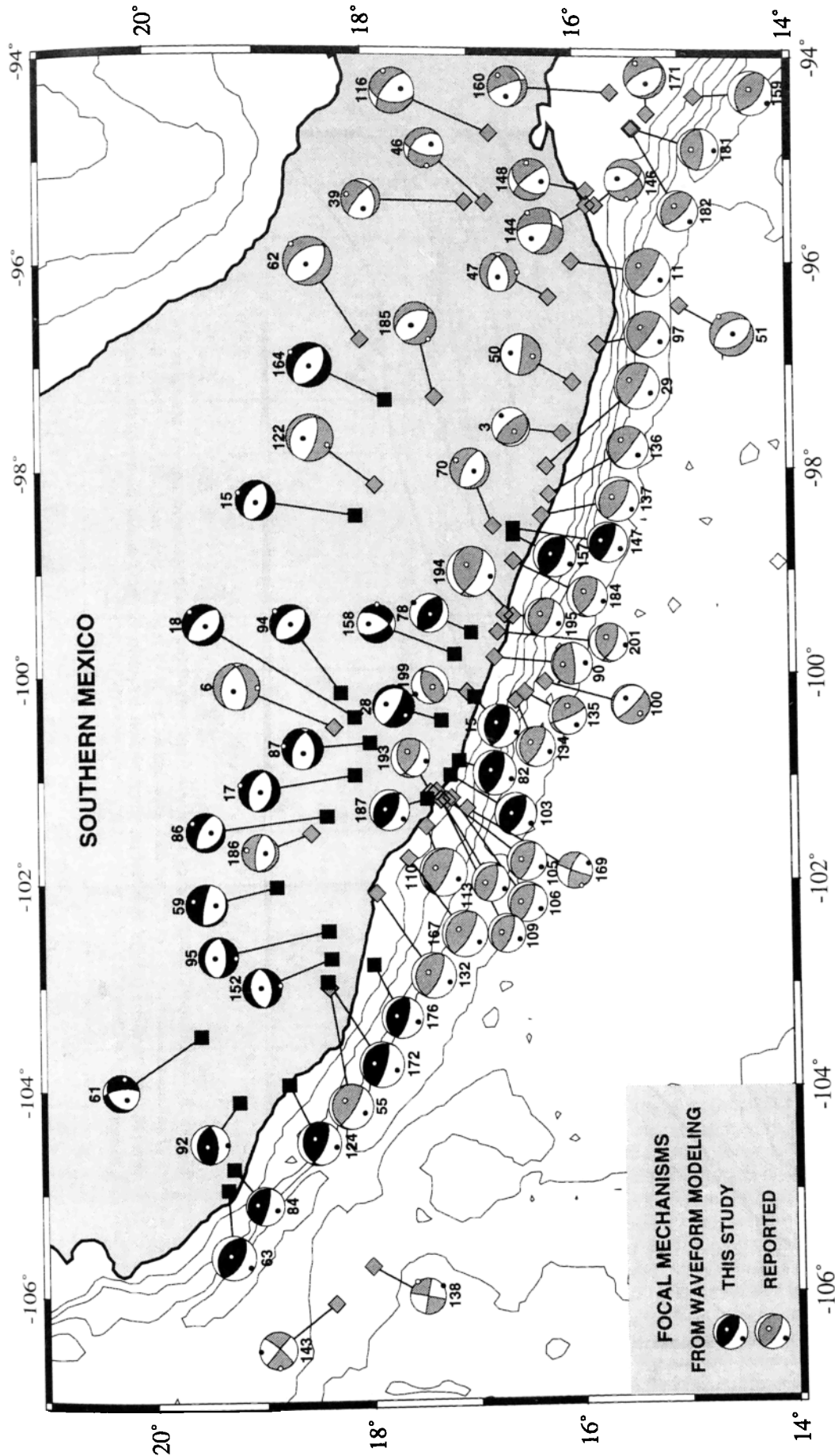


Figure 7. Focal mechanisms shown on lower hemispheric projection. Solid symbols are from the body wave inversion results reported in this study; the shaded symbols are from waveform modeling results reported elsewhere. *P* and *T* axes are shown on the mechanisms as black and white dots respectively. Numbers are keyed to those shown in the electronic supplement.

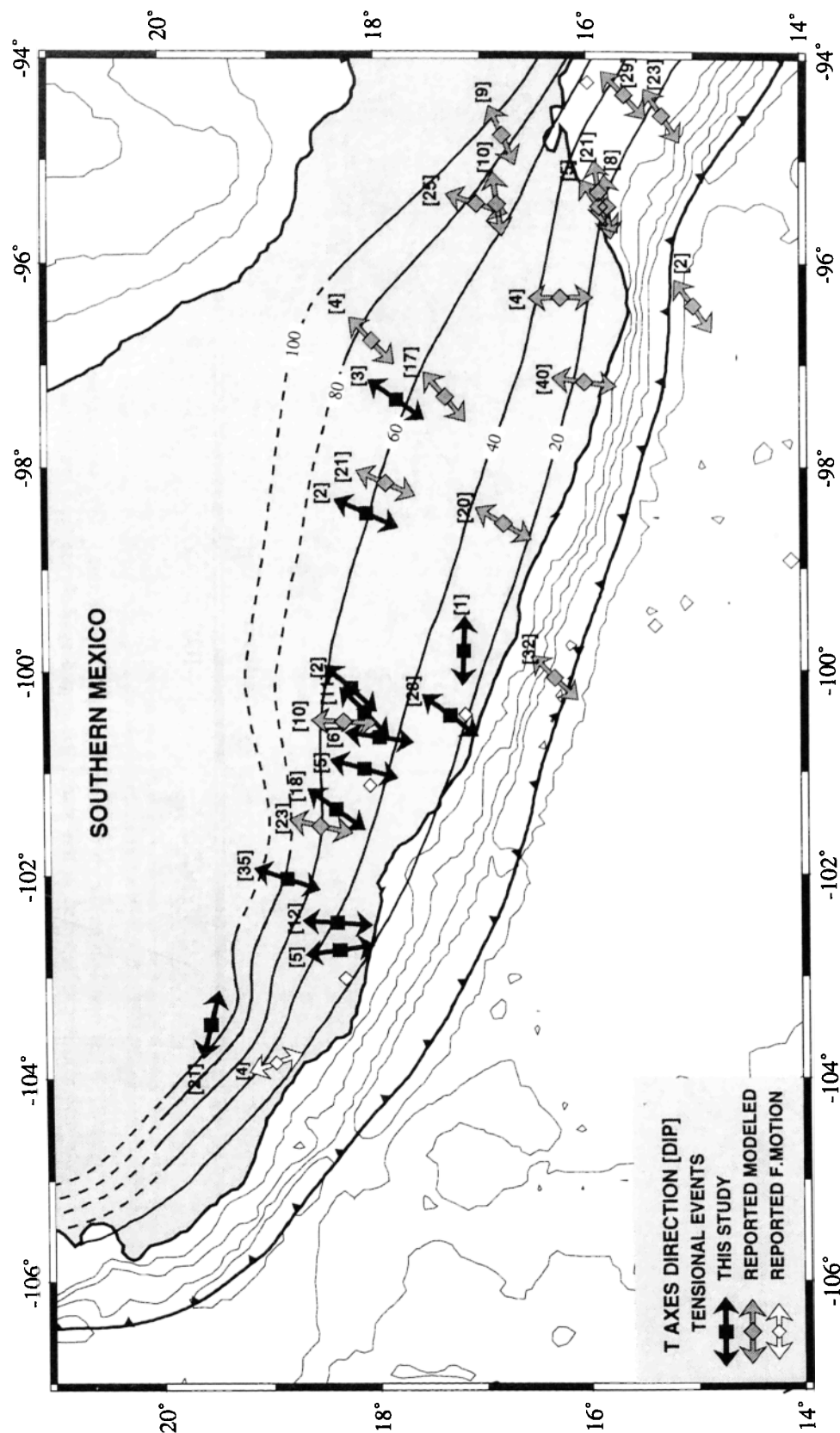


Figure 8. Orientation of the T axes obtained from waveform modeling; solid arrows are from focal mechanisms reported in this study and dark gray arrows are from reported focal mechanisms. Notice that, in general, the T axes are parallel to direction of subduction except in the areas where the dip of the subduction changes.

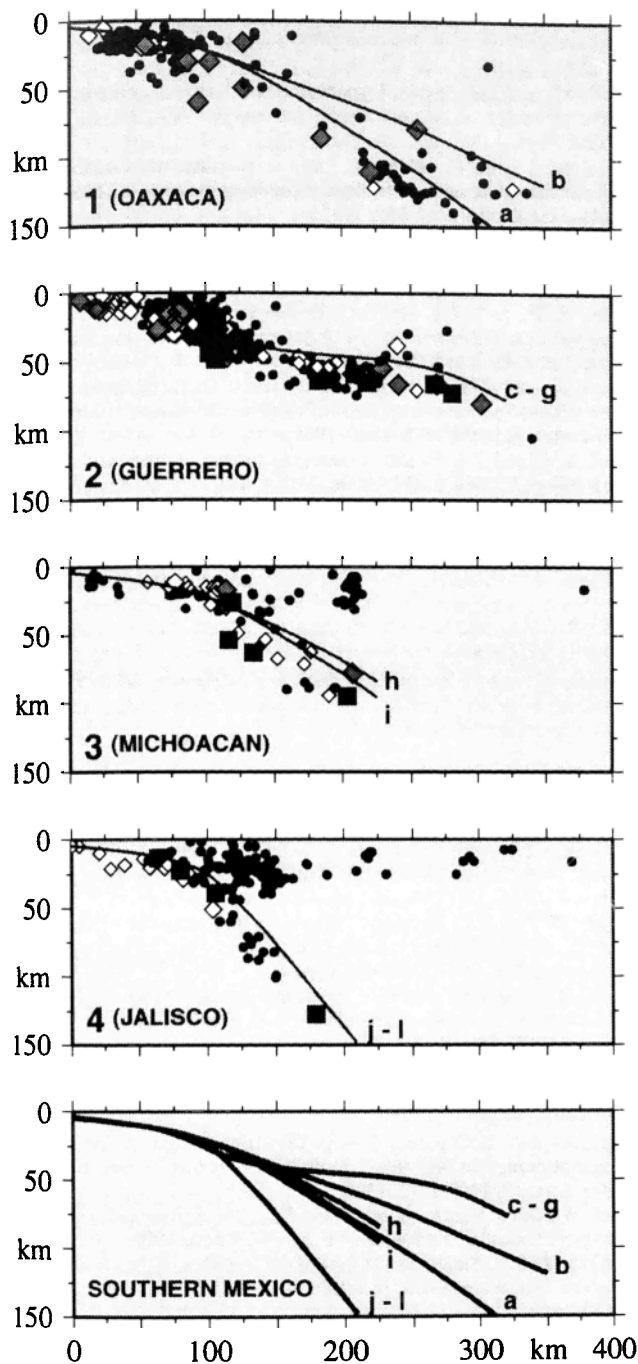


Figure 9. Comparison of the cross sections of the four regions into which southern Mexico was divided based on the seismicity and shape of the subduction zone. The seismicity and the plate geometry are a superposition of the cross sections on Figure 4, and are labeled with the same letters. The bottom figure shows a comparison of the geometry of subduction in each of these regions in southern Mexico.

Seismic and Tectonic Implications

The depth extent and dip of the interplate megathrust is constant and does not exhibit any clear correlation with the age of the subducted plate, with the relative convergence velocity, or with the subduction of bathymetric features along the trench (Figures 4 and 6). Thus the different rupture modes and complexity of the seismic sources reported for large thrust

earthquakes along the coupled interplate contact in southern Mexico [Singh and Mortera, 1991] is probably related to variations in the strength of coupling along the plate interface and not to the geometry of the subduction or to the depth extent of the coupled interplate zone.

The depth extent of the seismogenic plate contact can be estimated from the maximum depth of the shallow thrust earthquakes [e.g., Suárez and Comte, 1993]. In the case of the Cocos plate, this depth is consistently shallower than ~25 km. This results yield an unusually narrow seismogenic zone which is only ~60 km wide. This shallow depth of seismogenic coupling is about half as deep as that observed in most subduction zones of the world [e.g., Pacheco *et al.*, 1993].

In the case of the Rivera plate, the maximum depth of seismogenic coupling appears to be slightly deeper and reach ~40 km. This observation is suggested by a coastal earthquake showing a nodal plane dipping to the northeast at an angle of 34° (event 92 on Figure 4j and on the electronic supplement). If this earthquake still reflected the interplate contact, the width of the seismogenic zone of the Rivera plate would be wider (~75 km) than that of the Cocos plate, and, potentially, earthquakes of greater magnitude could be generated on its plate interface. Interestingly, the largest earthquake this century on the Middle American Trench, the 1932, Jalisco earthquake ($M_s=8.2$), occurred on the Rivera-North America plate interface [Eissler and McNally, 1984; Singh *et al.*, 1985].

The lateral variations in the dip angle of the subducted plate at depths greater than 30 km (Figure 4, 5, and 6) suggest that southern Mexico can be divided into four regions bounded approximately by major bathymetric features identified offshore (Figures 6 and 9). (1) The Jalisco region, where the steep-dipping Rivera plate subducts beneath North America is bounded to the east by the subduction of the El Gordo graben. In fact, the significant differences in the dip of the slab on both sides of the El Gordo graben may indicate that this tectonic feature decouples the downgoing Rivera and Cocos plates. (2) The Michoacan region, is a transition zone between the steep subduction of the Rivera plate and the almost subhorizontal subduction to the east. As mentioned before, it is bounded by the El Gordo graben to the west and by the onshore projection of the Orozco fracture zone to the east. (3) The Guerrero-Oaxaca region shows an almost subhorizontal geometry of the subducted Cocos plate. Geographically, this region can be defined as bounded by the Orozco and the O'Gorman fracture zones. (4) The southern Oaxaca region in southeastern Mexico is a transition zone between the flat subduction geometry beneath Guerrero and the steep subduction geometry of the Cocos plate beneath the Caribbean plate towards the east.

The remarkable absence of seismic events with depths greater than 70 km, north of ~18°N and of the Trans-Mexican Volcanic Belt suggests that the downgoing plate loses its brittle behavior and sinks aseismically into the mantle to the north of the volcanic belt. Perhaps low-magnitude earthquakes occur which are too small to be detected by the insufficient seismic network coverage that exists today. The inferred 80- and 100-km-deep contours of the downgoing slab appear to lie beneath the southern front of the Trans-Mexican Volcanic Belt (Figure 6). This observation strongly suggests the association of this volcanic belt with the subduction of the oceanic plate beneath the North American plate. Thus the

observed nonparallelism of the Trans-Mexican Volcanic Belt with the trench is mainly due to the geometry of the subducted Rivera and Cocos plates in southern Mexico.

Summary and Conclusions

The shape of the subducted Rivera and Cocos plates beneath the North American plate in southern Mexico was determined using accurately located hypocenters of earthquakes. A total of 1101 microearthquakes hypocenters recorded by local networks and 207 relocated hypocenters of earthquakes recorded at teleseismic distances were used as the database. For 21 teleseismic events ($m_b > 5.0$), the source parameters were determined using a formal long-period, body wave inversion [Nábelek, 1984]. In the relocation procedure [Dewey, 1971], the focal depth of these latter events was constrained by the inversion and used within the initial subset of events to generate the variance of the residuals at each teleseismic station, which were then applied to all the events in the relocation scheme.

The subduction in southern Mexico may be approximated as a subhorizontal slab subducting beneath the North American plate, which is bounded by a steep subduction geometry of the Cocos plate beneath the Caribbean plate to the east and the Rivera plate beneath the North American plate to the west. No lateral changes in the dip of the coupled interplate zone are observed at depths of less than 30 km. The changes in dip of the downgoing slab geometry are observed once it is decoupled from the overriding plate. The width of the seismogenic zone of the Rivera plate is apparently wider (~75 km) than that of the Cocos plate (~60 km).

The downgoing slab shows drastic changes in the dip angle, ranging from subhorizontal subduction beneath central Mexico to a relatively steep dip where the Tehuantepec ridge is being subducted. These changes in the dip of the downgoing slab do not appear to take place on tear faults, suggesting that smooth contortions accommodate these dip changes. The 80- and 100-km-depth contours of the subducted plate lie beneath the southern front of the Trans-Mexican Volcanic Belt, suggesting there is a direct association of this abnormally aligned volcanic belt with the complex subduction geometry of the subducted Rivera and Cocos plates in southern Mexico.

Acknowledgments. We thank the Servicio Sismológico Nacional, the Instituto de Geofísica, and the Instituto de Ingeniería, all of them at UNAM, and the Universidad de Colima for facilitating data from their local and temporary networks. We are grateful to S.K. Singh and J. Pacheco for helpful discussions and a review of the manuscript. The manuscript was greatly improved by comments made by D. E. James and an anonymous reviewer. Thanks are due to W.H.F. Smith and P. Wessel for the use of the program GMT to draft the figures. This research was partially supported by CONACYT and by project UACPyP-UNAM 30309. One of us (M.P.) acknowledges a fellowship from the Secretaría de Relaciones Exteriores, México.

References

- Allan, J.F., S.A. Nelson, J.F. Luhr, I.S.E. Charnichael, M. Wopat, and P.J. Wallace, Pliocene-Holocene rifting and associated volcanism in southwest Mexico: An exotic terrane in the making, in *The Gulf and Peninsular Provinces of the Californias*, edited by J.P. Dauphin and R.R.T. Simoneit, *AAPG Mem.*, 47, 425-445, 1991.
- Atwater, T., Implications of plate tectonics for the Cenozoic tectonic evolution of western North America, *Geol. Soc. Am. Bull.*, 81, 3513-3536, 1970.
- Bandy, W.L., Geological and geophysical investigation of the Rivera-Cocos plate boundary: Implications of plate fragmentation, Ph.D. thesis, Tex A&M Univ., College Station, 1992.
- Bandy, W.L., and C. Y. Yan, Present-day Rivera-Pacific and Rivera-Cocos relative plate motions (abstract) *Eos Trans. AGU*, 70, 1342, 1989.
- Bevis, M., and B.L. Isacks, Hypocentral trend surface analysis: Probing the geometry of Benioff zones, *J. Geophys. Res.*, 89, 6153-6170, 1984.
- Bourgeois, J., and F. Michaud, Active fragmentation of the North American plate at the Mexican triple-junction area off Manzanillo, *Geo Mar. Lett.*, 11, 59-65, 1991.
- Burbach, G., C. Frolich, W. Pennington, and T. Matumoto, Seismicity and tectonics of the subducted Cocos plate, *J. Geophys. Res.*, 89, 7719-7735, 1984.
- Chael, E. P., and G.S. Stewart, Recent large earthquakes along the middle American trench and their implications for the subduction process, *J. Geophys. Res.*, 87, 329-338, 1982.
- Couch, R., and S. Woodcock, Gravity and structure of the continental margins of southwestern Mexico and northwestern Guatemala, *J. Geophys. Res.*, 86, 1829-1840, 1981.
- Cross, R.H., and T.A. Pilger, Controls of subduction geometry, location of magmatic arcs, and tectonics of arc and back-arc regions, *Geol. Soc. Am. Bull.*, 93, 545-562, 1982.
- Dean, B.W., and C.L. Drake, Focal mechanism solutions and tectonics of the Middle America arc, *J. Geol.*, 86, 111-128, 1978.
- Delgado, H., P. Cervantes, and R. Molinero, Origen de la faja volcánica trans-mexicana hace 8.3 Ma y sus migraciones hacia el W, SW y SSW desde 5.3 Ma (abstract) *GEOS Unión Geofis. Mex.*, 13, 31-32, 1993.
- Demant, A., and C. Robin, Las fases del volcanismo en México; una síntesis en relación con la evolución geodinámica desde el Cretácico, *Rev. Inst. Geol., UNAM*, 75, 70-82, 1975.
- DeMets, C., and S. Stein, Present-day kinematics of the Rivera plate and implications for tectonics in southwestern Mexico, *J. Geophys. Res.*, 95, 21, 931-21, 948, 1990.
- DeMets, C., R.G. Gordon, D.F. Argus, and S. Stein, Current plate motions, *Geophys. Res. J. Int.*, 101, 425-478, 1990.
- Dewey, J.W., Seismicity studies with the method of joint hypocenter determination, Ph.D. thesis, Univ. of Calif., Berkeley, 1971.
- Eissler, H., and K.C. McNally, Seismicity and tectonics of the Rivera plate and implications for the 1932 Jalisco, Mexico, earthquake, *J. Geophys. Res.*, 89, 4520-4530, 1984.
- Gastil, R.G., and W. Jensky, Evidence for strike-slip displacement beneath the Trans-Mexican volcanic belt, *Stanford Univ. Publ. Geol. Sci.*, 13, 171-180, 1973.
- González-Ruiz, J., Earthquake source mechanics and tectonophysics of the middle America subduction zone in Mexico, Ph.D. thesis, Univ. of Calif., Santa Cruz, 1986.
- Gripp, A., and R. Gordon, Current velocities relative to the hotspots incorporating the NUVEL-1 global plate motion model, *Geophys. Res. Lett.*, 17, 1109-1112, 1990.
- Hanus, V., and J. Vanek, Subduction of the Cocos plate and deep active fracture zones of Mexico, *Geofis. Int.*, 17, 14-53, 1978.
- Havskov, J., S.K. Singh, and D. Novelo, Geometry of the Benioff zone in the Tehuantepec area in southern Mexico, *Geofis. Int.*, 21, 325-330, 1982.
- Jarrard, R.D., Relations among subduction parameters, *Rev. Geophys.*, 24, 217-284, 1986.
- Johnson, C.A., and C.G.A. Harrison, Tectonics and volcanism in central Mexico: A Landsat thematic mapper perspective, *Remote Sens. Environ.*, 28, 273-286, 1989.
- Klitgord, K., and J. Mammerrickx, Northern East Pacific Rise: Magnetic anomaly and bathymetric framework, *J. Geophys. Res.*, 87, 6725-6750, 1982.
- Lee, W.H.K., and C. Valdes, HYPO71PC: A personal computer version of the HYPO71 earthquake location program, *U.S. Geol. Surv. Open File Rep.* 85-749, 1985.
- LeFevre, L.V., and K.C. McNally, Stress distribution and subduction on aseismic ridges in the middle America subduction zone, *J. Geophys. Res.*, 90, 4495-4510, 1985.
- Luhr, J., S. Nelson, J. Allan, and I.S.E. Charnichael, Active rifting in southwestern Mexico: Manifestations of an incipient east-ward spreading-ridge jump, *Geology*, 13, 54-57, 1985.
- Mammerrickx, J., The morphology of propagating spreading centers: New and old, *J. Geophys. Res.*, 89, 1817-1828, 1984.
- Mammerrickx, J., and K. Klitgord, Northern East Pacific Rise: Evolution from 25 m.y.B.P. to the present, *J. Geophys. Res.*, 87, 6751-6759, 1982.
- Molnar, P., Fault plane solutions of earthquakes and direction of motion

- in the Gulf of California and on the Rivera Fracture zone, *Geol. Soc. Am. Bull.*, **84**, 1651-1658, 1973.
- Molnar, P., and L. R. Sykes, Tectonics of the Caribbean and Middle American region from focal mechanisms and seismicity, *Geol. Soc. Am. Bull.*, **80**, 1639-1684, 1969.
- Mooser, F., The Mexican volcanic belt: Structure and tectonics, *Geofis. Int.*, **12**, 55-70, 1972.
- Nábelek, J.L., Determination of earthquake source parameters from inversion of body waves, Ph.D. thesis, 346 pp., Mass. Inst. of Technol., Cambridge, 1984.
- Nava, E., Estudio de los temblores de Ometepe del 7 de Junio de 1982 y sus replicas, thesis, Univ. Nac. Autónoma de México, México D.F., 1984.
- Nixon, G. T., The relationship between Quaternary volcanism in central México and the seismicity and structure of subducted oceanic lithosphere, *Geol. Soc. Am. Bull.*, **93**, 514-523, 1982.
- Pacheco, J.F., L.R. Sykes, and C. H. Scholz, Nature of seismic coupling along simple plate boundaries of the subduction type, *J. Geophys. Res.*, **98**, 14,133-14,159, 1993.
- Pardo, M., and G. Suárez, Steep subduction geometry of the Rivera plate beneath the Jalisco block in western Mexico, *Geophys. Res. Lett.*, **20**, 2391-2394, 1993.
- Ponce, L., Gaulon, G. Suárez, and E. Lomas, Geometry and state of stress of the downgoing Cocos plate in the Isthmus of Tehuantepec, Mexico, *Geophys. Res. Lett.*, **19**, 773-776, 1992.
- Reyes, A., J. Brune, and C. Lomnitz, Source mechanism and aftershock study of the Colima, Mexico earthquake of January 30, 1973, *Bull. Seismol. Soc. Am.*, **69**, 1819-1840, 1979.
- Sansores, L., Sismicidad, esfuerzos y atenuación previos y posteriores al terremoto del 29-XI-1978, Oaxaca ($M_s=7.8$), thesis, Univ. Nac. Autónoma de México, México D.F., 1990.
- Shurbet, D.H. and S.E. Cebull, Tectonic interpretation of the Trans-Mexican volcanic belt, *Tectonophysics*, **101**, 159-165, 1973.
- Singh, S.K., and F. Mortera, Source time functions of large Mexican subduction earthquakes, morphology of the Benioff zone, age of the plate, and their tectonic implications, *J. Geophys. Res.*, **96**, 21,487-21,502, 1991.
- Singh, S.K., and M. Pardo, Geometry of the Benioff zone and state of stress in the overriding plate in central Mexico, *Geophys. Res. Lett.*, **20**, 1483-1486, 1993.
- Singh, S.K., L. Ponce, and S.P. Nishenko, The great Jalisco, Mexico, earthquake of 1932: Subduction of the Rivera Plate, *Bull. Seismol. Soc. Am.*, **75**, 1301-1313, 1985.
- Smith, W.H.F., and P. Wessel, Gridding with continuous curvature splines in tension, *Geophysics*, **55**, 293-305, 1990.
- Stoiber R.E., and M.J. Carr, Quaternary volcanic and tectonic segmentation of Central America, *Bull. Volcanol.*, **37**, 304-325, 1973.
- Suárez, G., and D. Comte, Comment on "Seismic coupling along the Chilean subduction zone" by B.W. Tichelaar and L.R. Ruff, *J. Geophys. Res.*, **98**, 15,825-15,828, 1993.
- Suárez, G., and S.K. Singh, Tectonic interpretation of the Trans-Mexican Volcanic Belt-Discussion, *Tectonophysics*, **127**, 155-160, 1986.
- Suárez, G., T. Monfret, G. Wittlinger, and C. David, Geometry of subduction and depth of the seismogenic zone in the Guerrero gap, Mexico, *Nature*, **345**, 336-338, 1990.
- Suárez, G., J.P. Ligorria, and L. Ponce, Preliminary crustal structure of the coast of Guerrero, Mexico, using the minimum apparent velocity of refracted waves, *Geofis. Int.*, **31**, 247-252, 1992.
- UNAM Seismology Group, The September 1985 Michoacan earthquakes: Aftershock distribution and history of rupture, *Geophys. Res. Lett.*, **13**, 573-576, 1986.
- Valdés, C., R. Meyer, R. Zúñiga, J. Havskov, and S.K. Singh, Analysis of the Petatlan aftershocks: Numbers, energy release and asperities, *J. Geophys. Res.*, **87**, 8519-8529, 1982.
- Zúñiga, F.R., C. Gutierrez, E. Nava, J. Lermo, M. Rodríguez and R. Coyoli, Aftershocks of the san Marcos earthquake of April 25, 1989 ($M_s=6.9$) and some implications for the Acapulco-San Marcos seismic potential, *Pure Appl. Geophys.*, **140**, 287-300, 1993.

M. Pardo, Departamento de Geofísica, Universidad de Chile, Casilla 2777, Santiago, Chile. (e-mail: mpardo@dgf.uchile.cl)

G. Suárez, Instituto de Geofísica, Universidad Nacional Autónoma de México, Apartado Postal 70-172, México D.F., México. (e-mail: gerardo@ollin.igeof.unam.mx)

(Received July 7, 1994; revised March 1, 1995;
accepted March 16, 1995.)